

Modification of titanium implants using biofunctional nanodiamonds for enhanced antimicrobial properties

Emilia Krok^{1,2,3,5} , Sascha Balakin^{1,4} , Jonas Jung⁴ , Frank Gross², Jörg Opitz^{1,4,5}  and Gianaurelio Cuniberti⁴ 

¹ Bio- and Nanotechnology, Fraunhofer Institute for Ceramic Technologies and Systems IKTS Material Diagnostics, Dresden, Germany

² Biotechnology Center (BIOTEC) of Technische Universität Dresden, Dresden, Germany

³ Poznań University of Technology, Faculty of Physics, Institute of Molecular Physics, Poznań, Poland

⁴ Institute for Materials Science and Max Bergmann Center of Biomaterials, Technische Universität Dresden, Dresden, Germany

E-mail: emilia.krok@put.poznan.pl and joerg.opitz@ikts.fraunhofer.de

Received 14 October 2019, revised 12 December 2019

Accepted for publication 20 January 2020

Published 2 March 2020



Abstract

The present study describes a novel antimicrobial surface using anodic oxidation of titanium and biofunctional detonation nanodiamonds (ND). ND have been loaded with antibiotics (amoxicillin or ampicillin) using poly(diallyldimethylammonium chloride) (PDDA). Successful conjugation with PDDA was determined by dynamic light scattering, which showed increase in the hydrodynamic diameter of ND agglomerates and shift of zeta potential towards positive values. The surface loading of amoxicillin was determined using UV–vis spectroscopy and the maximum of 44% surface loading was obtained. Biofunctional ND were immobilized by anodic oxidation within a titanium oxide layer, which was confirmed by scanning electron microscopy. The *in vitro* antimicrobial properties of ND suspensions were examined using Kirby-Bauer test with *E. coli*. Modified titanium surfaces comprising biofunctional ND were evaluated with *E. coli* inoculum by live/dead assay staining. Both biofunctional ND suspensions and modified titanium surfaces presented inhibition of bacteria growth and increase in bacteria lethality.

Keywords: detonation nanodiamond, biomaterial, bone implant, antimicrobial surface, antibiotic

(Some figures may appear in colour only in the online journal)

1. Introduction

One of the major problem arising from orthopaedic implant surgery is the possibility of microbial infection, which leads to inflammation and loosening of the implant-bone connection. The most effective way to protect the patient from microbial infection is by preventing the biofilm formation onto the implant surface [1, 2]. The biofilm consists of polymers called extracellular polymeric substances, which not only form a bacterial habitat, but also create a protective layer against the antibiotics, UV radiation, dehydration, and host natural immunity [2]. The biofilm increases the bacterial

survival in antibiotics 100–1000 times higher concentrations than the normal dosage necessary to inhibit freely swimming bacteria [3]. In order to prevent *in vivo* bacteria attachment and development, a high concentration of antibiotic can be directly applied in the place of implantation combined with intravenous administration antimicrobial agents after the procedure [4–6]. In the commercial applications the antibiotic immobilization is utilized by addition of antibacterial agents to the bone cement. In this case, bone cement can act as a drug delivery system with localized release directly to the affected tissue. Antimicrobial agents such as gentamycin, tobramycin, erythromycin, vancomycin, and colistin have been added to the bone cement without any effect on its mechanical properties [7]. However, the use of bone cement

⁵ Authors to whom any correspondence should be addressed.

as a fixation material between implant and bone often leads to implant loosening due to the constant cycling loading, fatigue and shear forces which lead to the bone degradation at the cement-bone interface [8]. This creates a strong need for new immobilization techniques of antibiotics onto the implant surface. The covalent bonding of Vancomycin on the Ti surface was performed by Antoci *et al* [9]. However, the formation of covalent bond changes the structure and conformation of active sites in the molecule. This reorientation of functional groups influences the active sites especially in small molecules, which can lead to the loss of component activity [10]. Used in the above mentioned research vancomycin with its molecular weight 1449.2 Da can be considered as a big molecule. In case of amoxicillin and ampicillin, with molecular weight of 365.4 Da and 349.4 Da respectively, covalent bonding involving COOH group occurs close to the active beta lactam ring which leads to conformational changes of these antibiotics and to the suppressed mechanism of work.

In recent years, the focus on nanoparticles and nanodevices has advanced a wide range of biomedical applications: drug delivery, bioimaging, diagnostics, therapy, and tissue engineering [11–14]. Among the nanomaterials detonation nanodiamonds (ND) have attracted considerable interest as a potential platform for delivery of antibiotics due to their high biocompatibility, low cytotoxicity, and presence of various functional surface groups, which give numerous conjugation possibilities with different drugs [12, 15, 16]. As reported by Grausova *et al* nanostructured nanocrystalline diamond (NCD) films promote growth and differentiation of human osteoblast like MG 63 cells [17]. Authors presented increased cell proliferation and viability when compared to both flat and rough silicon substrates, polystyrene culture dishes and microscopic glass coverslips and proposed that incorporation of NCD films onto Ti implant surfaces can lead to improved osseointegration.

ND have been studied with regards to their antibacterial properties in pristine form or upon conjugation with antibiotics as potential antimicrobial agents [18]. Wehling *et al* examined the antibacterial properties of ND on Gram-negative *Escherichia coli* and Gram-positive *Bacillus subtilis*, presenting that ND at concentration of 0.05 mg ml^{-1} possess the same antibacterial properties as silver nanoparticles [19]. Lee *et al* conjugated ND with amoxicillin for gutta-percha root canal therapy. The loaded gutta-percha exposed to *Staphylococcus aureus* resulted in bacterial death, while unmodified gutta-percha did not present an increase in bacteria lethality [20]. Rouhani *et al* performed amoxicillin loading onto polyethyleneimine (PEI) functionalized ND with stronger binding, obtaining by this resistant to multiple washing steps conjugate [21]. However, this research did not give any qualitative analysis of the antimicrobial properties of prepared ND-PEI-amoxicillin conjugates.

In this work we propose a method for electrostatic loading of amoxicillin and ampicillin onto the ND surface, by using Poly(diallyldimethylammonium chloride) (PDDA) with further immobilization of the biofunctional ND within the titanium (Ti) oxide layer (figure 1). The modified Ti surfaces were analyzed with *E. coli* and were found to exhibit

strong antimicrobial properties by causing contact-mediated bacteria lethality.

2. Materials and methods

2.1. Reagents and chemicals

ND with average particle size of 4 nm were used for all experiments and purchased from PlasmaChem GmbH, Berlin, Germany. Sodium hydroxide ($M_{\text{NaOH}} = 40.0 \text{ g mol}^{-1}$) and potassium chloride ($M_{\text{KCl}} = 74.6 \text{ g mol}^{-1}$) were obtained from Carl Roth GmbH Co. KG, Karlsruhe, Germany. The Poly(diallyldimethylammonium chloride) (PDDA) solution 20 wt% in H_2O , amoxicillin with potency $\geq 900 \mu\text{g mg}^{-1}$ ($M_{\text{amoxicillin}} = 365.4 \text{ g mol}^{-1}$) and ampicillin 96%–102% (anhydrous basis) ($M_{\text{ampicillin}} = 349.4 \text{ g mol}^{-1}$) were purchased from Sigma-Aldrich, St. Louis, MO, USA. The ultrapure water (ddH_2O) was obtained by using Direct-Q® Water Purification UV System from Merck KGaA, Darmstadt, Germany. Phosphate-buffered saline (PBS) was purchased from Merck KGaA, Darmstadt, Germany. The ceramic grinding beads type ZY-P (yttrium stabilized zirconia) with a diameter of $100 \mu\text{m}$ were purchased from Sigma Linder GmbH, Warmensteinach, Germany. Commercially pure titanium (cp-Ti) discs grade 4 were obtained from DOT GmbH, Rostock, Germany. A salt bridge for anodization was prepared by using the capillary plastic tube Tygon® LMT-55 from Pro Liquid GmbH, Überling, Germany. Petri dishes with LB Lennox agar (pH 7.5) were obtained from BIOTEC Dresden Genomics facility. Antimicrobial experiment were performed using *E. coli* GB05 and *E. coli* K12. The Live/Dead BacLight Bacterial Viability Kit for microscopy (L7007) was purchased from Invitrogen Thermo Fischer Scientific, Waltham, Massachusetts, USA.

2.2. ND suspension preparation

In order to obtain stable and homogenous ND suspensions two types of homogenization techniques were applied. One group of NDs suspensions was exposed only to sonication (indicated as ND*) and second group was treated with bead milling and sonication (indicated as ND). Bead-milling was performed by using the planetary micro mill Pulverisette 7 from Fritsch GmbH, Idar-Obenstein, Germany. In brief, each of two grinding bowls was filled with 15 ml of ddH_2O , 0.75 g of pristine ND, and 7.5 g of grinding beads. The milling was performed in two cycles at 700 rpm, for 30 min for each cycle with 10 min break in between. Grinding beads were removed from ND by filtration. Bead-milled ND were diluted using ddH_2O to final concentrations of 1 mg ml^{-1} and 0.5 mg ml^{-1} . The suspensions were stabilized by pH adjustment using NaOH [22]. After pH adjustment, the solutions were additionally exposed to 30 min of ultrasonic treatment using Sonoplus HD 2200 ultrasonic homogenizer from Bandelin electronic GmbH and Co. KG, Berlin, Germany at 70% of the device power. For the samples exposed only to sonication, bead-milling step was not applied.

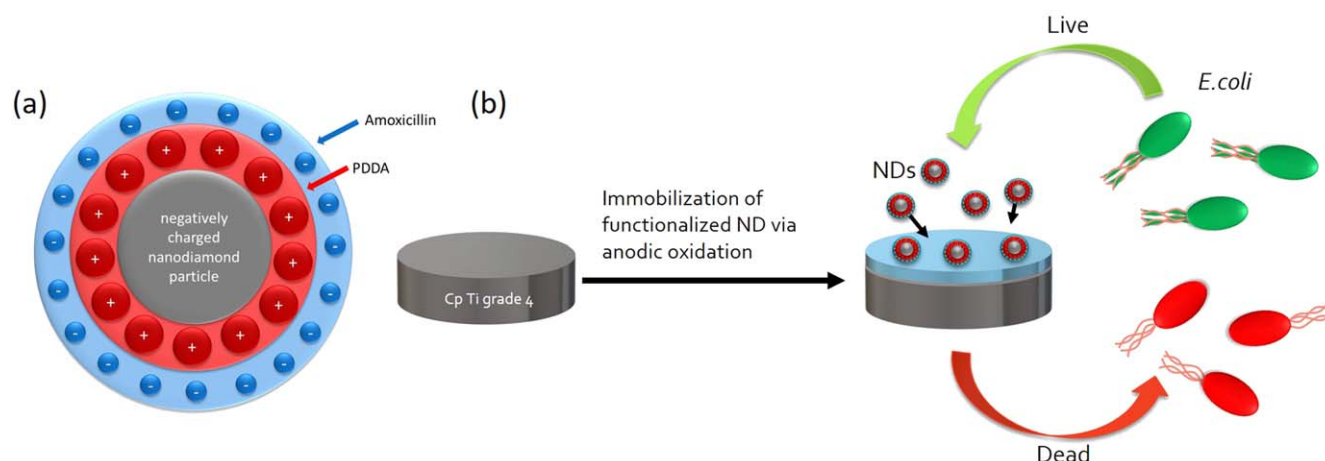


Figure 1. Schematic representation of the: (a) biofunctional ND utilizing PDDA/amoxicillin. The conjugation was based on the electrostatic interactions. Bare ND with negative charge (gray core) was conjugated with positively charged PDDA (red layer) and further with negatively charged amoxicillin (blue layer), (b) immobilization of biofunctional NDs on the surface of the commercially pure Ti grade 4 by using anodic oxidation. *E. coli* exposed to the modified surface presented the increased rate of lethality

2.3. ND conjugation with poly(diallyldimethylammonium chloride) and antibiotic agents

A volume of 20 ml ND in concentrations of 1 mg ml^{-1} and 0.5 mg ml^{-1} was mixed with 20 ml of 20 mg ml^{-1} and 10 mg ml^{-1} PDDA, respectively. The suspensions were further exposed to ultrasound (US) water bath for 30 min. The obtained suspensions were equally distributed into $10 \times 2 \text{ ml}$ microcentrifuge tubes. Centrifugation was done using high-speed centrifuge at 15,000 rpm for 30 min. After centrifugation, the supernatant was removed and each pellet was resuspended in 2 ml of ddH₂O. Washing was repeated two times. After the last washing step, the pellet was resuspended in 2 ml ddH₂O and all solutions were collected.

Amoxicillin was suspended in ddH₂O to obtain the final concentration of 1 and 0.5 mg ml^{-1} . Washed and PDDA functionalized ND pellets were resuspended in the corresponding concentrations of amoxicillin for 1:1 ratio. Samples were incubated on the rotary shaker for 1 h and for 9 days to compare the binding affinity of amoxicillin. Subsequently, ND suspensions were distributed into microcentrifuge tubes and centrifuged at 15,000 rpm for 30 min. The supernatant was collected to determine the amount of unbound amoxicillin by ultraviolet–visible spectroscopy (UV–vis). The area under the curve (AUC) spectra for amoxicillin in water were recorded at the wavelength range of 257–289 nm and the calibration curve was used to determine an unknown concentration from the solutions. The same functionalization procedure has been applied to conjugate ampicillin with the NDs.

2.4. Characterization of functionalized ND suspensions

ND and ND* agglomerate size and zeta potential were measured using dynamic light scattering (DLS) from Zetasizer Nano by Malvern Panalytical, Kassel, Germany with folded Capillary Zeta Cell DTS1070 made of polycarbonate with gold plated beryllium/copper electrodes. Before each

measurement ND and ND* suspensions were exposed to ultrasound water bath for 30 min. To determine the long term stability of the suspensions, the experiment was repeated one month later, but this time without applying ultrasound water bath right before the measurements. The surface loading of ND was determined using UV–vis–NIR Spectrophotometer Shimadzu UV-3600 Plus with deuterium lamp for UV measurements and Tungsten halogen for work in the visible light range.

2.5. ND immobilization within Ti oxide layer via anodic oxidation

The electrolyte for anodization with pH 12.1 was prepared according to the method described by Aliasghari *et al* [23]. The three-electrode system designed by Michael *et al* at Max Bergmann Center for Biomaterials was used for Ti anodization [24]. Each Ti disc (\varnothing 15 and 2 mm height) was cleaned with ethanol and placed inside the conically shaped chamber made of acrylic glass, which was filled with 1.5 ml of electrolyte and 1.5 ml of biofunctional ND. The working electrode was attached to the bolt to maintain the contact with the sample from below. From the top, the chamber was closed by a lid with attached platinum wire which acted as a counter electrode. The reference electrode was immersed in a borosilicate glass beaker containing 3M KCl solution. The silver chloride electrode was used as a reference for the potential measurement. The salt bridge was prepared by using the capillary plastic tube which was filled with 2% w/v in 2 mol l^{-1} borate buffer agarose gel, pH 7.4.

The anodic oxidation was performed under the galvanostatic mode. The current density was adjusted to 100 A m^{-2} with target potential of 90 V. After each anodization process, the Ti sample was removed and cleaned with ethanol. The topography was determined by using field emission scanning electron microscopy (SEM) JSM-7500F from JEOL Ltd, Tokyo, Japan.

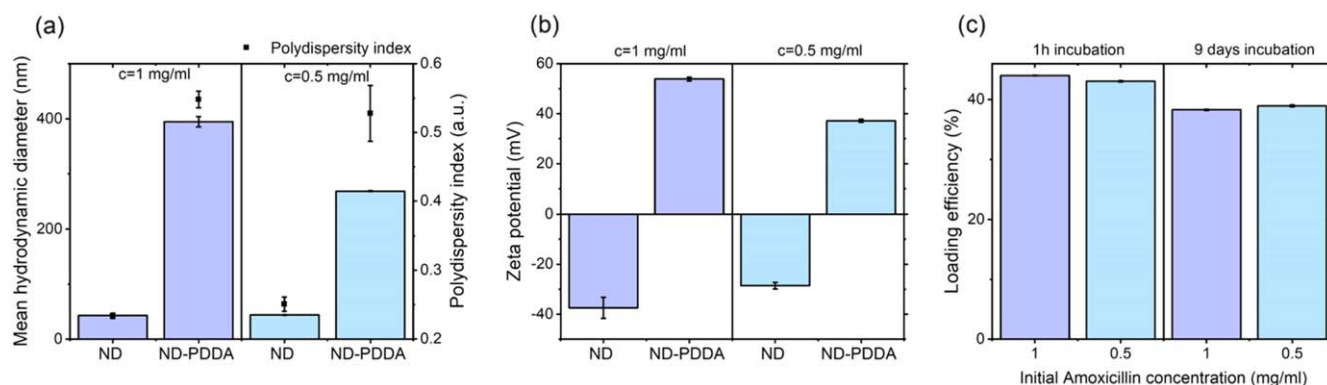


Figure 2. (a) Hydrodynamic diameter and (b) zeta potential of ND agglomerates functionalized with PDDA. (c) Surface loading of amoxicillin onto ND after 1 h and 9 days of incubation.

2.6. Antimicrobial testing

E. coli was grown in Lysogeny Broth (LB) medium in thermomixer, 950 rpm, under aerobic conditions at 37 °C until the log phase was reached. The inoculum was diluted to obtain 1.5×10^8 cells ml^{-1} , which corresponds to the 0.5 McFarland Turbidity Standard. Standard absorbance of bacteria suspension was measured at 600 nm by using Ultrospec 2100 pro from Amersham Biosciences, Little Chalfont, UK. A volume of 100 μl of the as-prepared bacteria suspension was pipetted in the middle of the agar plate. Cells were equally distributed on the plate using a spatula.

Discs for the Kirby-Bauer Test were made out of Whatman paper by cutting it with a puncher to obtain standard diameter of 6 ± 0.5 mm (ISO Standard 838 [25]) and autoclaved in aluminum foil at 121 °C for 30 min. Subsequently, the discs were soaked in one of the following solutions: ddH₂O (negative control), ND 1 mg ml^{-1} , ND-PDDA-amoxicillin 1 mg ml^{-1} , ND-PDDA-amoxicillin 0.5 mg ml^{-1} , amoxicillin 1 mg ml^{-1} (positive control) and ampicillin 100 μg ml^{-1} (positive control). Agar plates with *E. coli* and the discs was incubated for 24 h at 37 °C.

In order to evaluate the antibacterial properties of the respective surface, Ti samples were prepared possessing different surface modifications: (1) as-received Ti, (2) Ti exposed to anodic oxidation, oxidized Ti possessing (3) pristine ND, (4) ND functionalized with amoxicillin and (5) ampicillin. Ti samples were placed in 12-well microliter plates and 2 ml of bacteria inoculum was added. Samples were incubated for 24 h at 37 °C.

The amount of living and dead bacteria on the Ti samples was determined using the staining kit. Optical imaging was conducted using the reflected-light microscope Axio Scope Vario from Carl Zeiss Microscopy, Jena, Germany with both red and green emission filters. Quantification of the bacteria staining solutions was performed using microplate reader Infinite M200 Pro from Tecan Group Ltd, Zürich, Switzerland. SEM imaging of bacteria attached to Ti surfaces was performed on an environmental scanning electron microscope from Philips XL30 FEG, Hillsboro, OR, USA. Surface coverage upon exposure to *E. coli* inoculum was calculated based on the SEM images. The original images were converted to

black and white binary versions by adjusting the threshold of contrast in the ImageJ software [26]. Three different locations were chosen for determination of the area occupied by the bacteria cells.

3. Results and discussion

3.1. Characterization of functionalized ND suspensions

Formation of ND-PDDA-amoxicillin complex was assessed at each step of conjugation. ND suspensions were measured by DLS to determine the mean hydrodynamic diameter. As presented in figures 2(a) and (b) ND suspensions with a concentration 1 mg ml^{-1} had a hydrodynamic diameter of 43 ± 1 nm and a zeta potential of -38 ± 4 mV. ND with concentration 0.5 mg ml^{-1} had a hydrodynamic size of 44 ± 1 nm and a zeta potential -29 ± 1 mV. The results are consistent with the values reported in literature [22, 27]. After conjugation with PDDA, the hydrodynamic diameter of the 1 mg ml^{-1} sample increased to 395 ± 9 nm and zeta potential shifted to positive value of 54 ± 1 mV. Samples with concentration of 0.5 mg ml^{-1} upon conjugation with PDDA had a hydrodynamic diameter 268 ± 1 nm and a zeta potential 37 ± 1 mV. Che *et al* reported increase in the hydrodynamic diameter from 234.7 to 299.2 nm upon conjugation of silica with PDDA and change of zeta potential from -57 to 56.6 mV [28]. The observed increase of the mean hydrodynamic diameter after conjugation with PDDA, as well as the change of zeta potential to the positive values, indicated the successful functionalization of NDs with PDDA. All of the suspensions were within the stability range of zeta potential ≥ 30 mV [29].

In order to determine the concentration of amoxicillin UV/Vis spectroscopy is broadly used [30–32]. As reported by Ataklti *et al* two characteristics absorbance maxima were recorded for amoxicillin at 228 nm and at 278 nm [30]. Lee *et al* used maximum the absorbance value 270 nm for the determination of the calibration curve [20]. In order to increase the precision of the obtained results, the AUC method was used [33–35]. The amount of the loaded amoxicillin was calculated by subtracting the concentration of

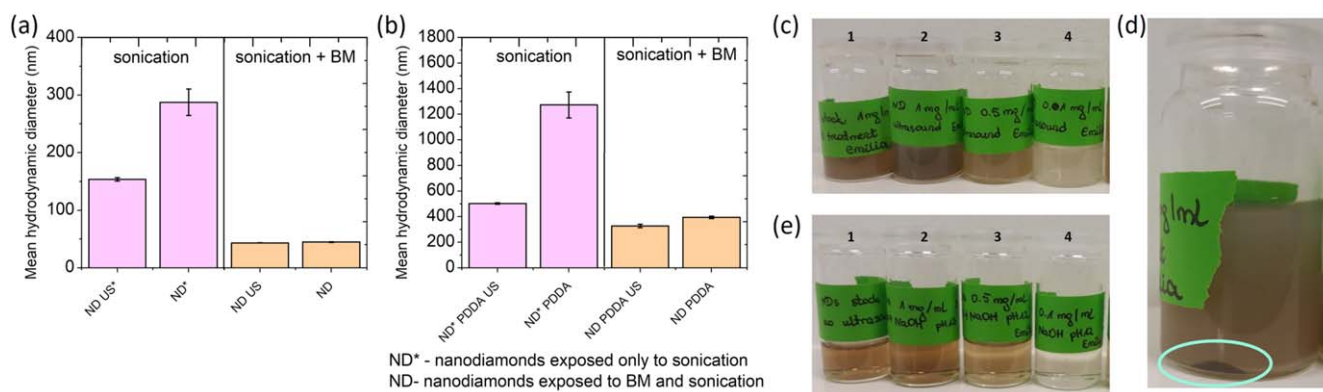


Figure 3. Particle size expressed by intensity of (a) samples exposed to US treatment right before the measurements (ND US and ND* US), and samples upon one month of storage and no US treatment applied before measurements (ND and ND*), (b) Samples upon conjugation with PDDA. (c) ND* suspensions stability: (1) stock 1 mg ml^{-1} without applied sonication, (2) 1 mg ml^{-1} , (3) 0.5 mg ml^{-1} , (4) 0.1 mg ml^{-1} , (d) Sample containing 1 mg ml^{-1} ND suspension after 1 h of storage, precipitation of ND on the bottom of the flask marked with cyan circle, (e) ND suspensions stability: (1) stock 1 mg ml^{-1} without sonication, (2) 1 mg ml^{-1} , (3) 0.5 mg ml^{-1} , (4) 0.1 mg ml^{-1}

recovered amoxicillin from the initial concentration. As shown in figure 2(c) after 1 h incubation with amoxicillin, $440 \pm 0.54 \mu\text{g ml}^{-1}$ and $215 \pm 0.47 \mu\text{g ml}^{-1}$ were loaded onto 1 mg ml^{-1} and 0.5 mg ml^{-1} of ND respectively, which corresponds to a surface loading of $44 \pm 0.1\%$ and $43 \pm 0.1\%$. After 9 days of incubation $382 \pm 1 \mu\text{g ml}^{-1}$, and $194 \pm 1 \mu\text{g ml}^{-1}$ were loaded onto 1 mg ml^{-1} and 0.5 mg ml^{-1} of ND respectively. The longer incubation time of 9 days did not increase the surface loading of amoxicillin onto ND and resulted in values lower than 40%. From these results PDDA-mediated conjugation of ND with amoxicillin is a very rapid process, based on electrostatic rather than chemical interactions, with PDDA as a bridging agent between negatively charged ND and positively charged amoxicillin [28, 36]. The maximum of 44% of surface loading was reached already after 1 h, and no further molecules were able to reach the surface due to steric repulsion [37]. The longer incubation time led to the renewed drug release from the NDs surface into the solvent based on the dissociation processes. However, the lowest concentration loaded onto ND was still higher than the minimum inhibitory concentration for *E. coli* ($2 \mu\text{g ml}^{-1}$) and *S. aureus* ($0.12 \mu\text{g ml}^{-1}$) [38]. The antimicrobial properties of our conjugates are determined by the stability and activity of amoxicillin in solution, which is known to be stable for 7–14 d in water [39, 40].

The stability testing of ND suspensions was utilized by DLS. As shown in figure 3(a) the mean hydrodynamic diameter was $154 \pm 3 \text{ nm}$ and $43 \pm 1 \text{ nm}$ for sample exposed only to sonication (ND*) and sample treated with both sonication and bead-milling (ND) respectively. Upon one month of storage it was observed that ND* presented significant increase in the mean hydrodynamic diameter to value of $288 \pm 23 \text{ nm}$. ND suspensions did not show the increase in the agglomerate size upon storage, resulting in the mean hydrodynamic diameter of $45 \pm 1 \text{ nm}$. It was observed that exposure of ND only to the sonication treatment was not sufficient to obtain desired particle size due to the strong agglomeration of ND. The same methodology was applied upon conjugation with PDDA. As shown in figure 3(b), due

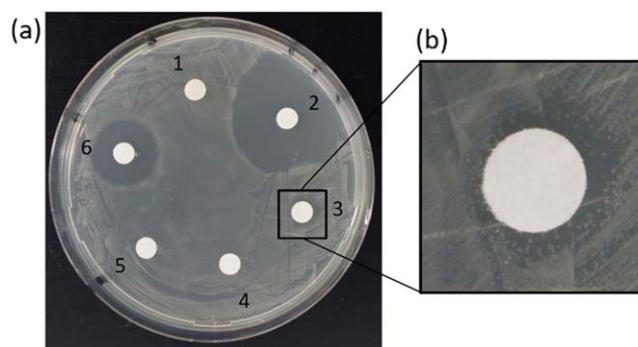


Figure 4. Kirby-Bauer Test against *E. coli* GB05 to evaluate the antibacterial properties of the ND suspension. (a) Inhibition zones of (1) pristine ND 1 mg ml^{-1} , (2) ampicillin $100 \mu\text{g ml}^{-1}$ (positive control), (3) ND-PDDA-amoxicillin 1 mg ml^{-1} , (4) ND-PDDA-amoxicillin 0.5 mg ml^{-1} , (5) ddH₂O (negative control), (6) amoxicillin 1 mg ml^{-1} (positive control) and (b) magnified image of the inhibition zone for ND-PDDA-amoxicillin 1 mg ml^{-1} .

to the one month storage, samples conjugated with PDDA, exposed only to sonication presented increase of mean hydrodynamic diameter from 503 ± 6 to $1273 \pm 102 \text{ nm}$. Samples that were treated with both sonication and bead milling also reagglomerated but with lower rate from $328 \pm 13 \text{ nm}$ to $395 \pm 9 \text{ nm}$ upon one month storage. The strong aggregation upon conjugation with PDDA was observed for the samples exposed only to sonication. Samples that underwent both bead milling and sonication presented long term stability even in the presence of PDDA. Moreover no reagglomeration was observed in case of the samples exposed only to sonication. Furthermore as presented in figure 3(c) the lack of stability for the samples exposed only to sonication was observed by bare eye. These suspensions were blurry and, even upon as short time as 1h of storage, the precipitation of ND was observed on the bottom of the flask as shown in figure 3(d). ND that were additionally treated with bead milling procedure presented clear brownish color as shown in figure 3(e), and could be stored for few months

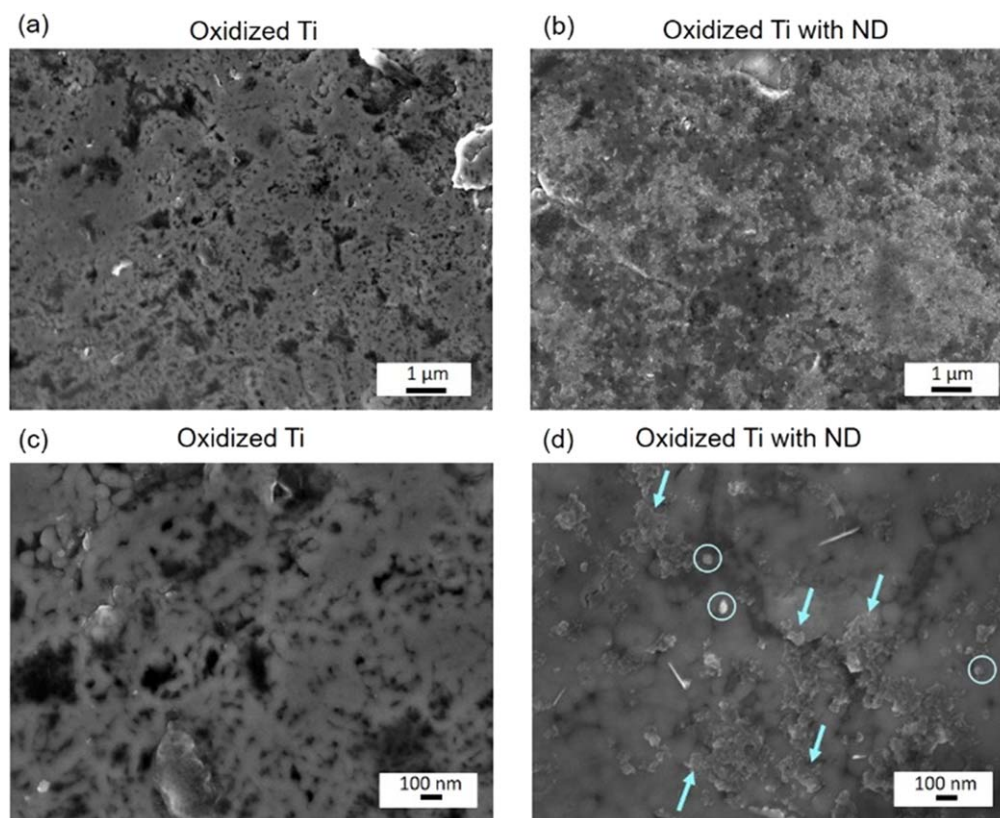


Figure 5. SEM images of (a) Ti surface exposed to anodic oxidation and (b) Ti surface with immobilized ND within the oxide layer, (c) magnified zone of Ti oxidized, (d) magnified zone of Ti with immobilized ND. ND agglomerates are marked by arrows and single ND agglomerates are highlighted in the circles.

without any changes in the stability. We also did not observe any precipitation or reagglomeration, based on the DLS measurements performed after 1 month of storage.

3.2. Evaluation of antimicrobial properties of ND conjugates in suspension

The antimicrobial properties of the ND-PDDA-amoxicillin conjugates in suspension were evaluated using the Kirby-Bauer test. The results from the Kirby-Bauer test with *E. coli* GB05 are presented in figure 4(a). Two large inhibition zones were observed for both positive control groups: 1 mg ml⁻¹ amoxicillin and 100 μg ml⁻¹ ampicillin, with the largest inhibition observed for ampicillin. No inhibition zone was observed around water negative control, pristine ND 1 mg ml⁻¹, and ND-PDDA-amoxicillin 0.5 mg ml⁻¹. The disc soaked in ND-PDDA-amoxicillin 1 mg ml⁻¹ showed a small inhibition zone (figure 4(b)). The lack of inhibition zone for pristine ND is consistent with the findings of Lee *et al* [20]. As reported by Kourmouli *et al* the diffusion rate of nanoparticles with a diameter greater than 10 nm is more than one order of magnitude lower than the diffusivity of commonly used antibiotics [41]. The ND cannot diffuse from the paper discs to the agar and no direct interaction of the bio-functional ND with the bacteria cell walls are possible. Therefore, the observed inhibition zones are strongly dependent on the ions or antibiotic release from ND surface and not a result from ND diffusion. Hence, the inhibition zone visible

for ND-PDDA-amoxicillin conjugates, was the result of breaking the electrostatic interactions between PDDA and amoxicillin subsequently releasing amoxicillin into agar.

3.3. Topography of oxidized Ti with immobilized ND

ND have been immobilized within Ti oxide layer using anodic oxidation and the topography has been assessed by SEM. Figure 5 displays the SEM images of the Ti surfaces. The surface of the oxidized Ti without addition of ND was recorded as reference material and is shown in figures 5(a) and (c). Once ND are employed in the electrolyte the oxidized Ti surface shows nanoscale features as presented in figure 5(b). As shown in figure 5(d), ND formed dense clusters of agglomerates of around 40–50 nm, which was consistent with the values obtained from DLS measurements for ND solutions. The successful immobilization supports the previous findings reported in our group by Gonçalves *et al* [42].

3.4. Antimicrobial properties of modified Ti surfaces

To examine the antimicrobial properties of the functionalized Ti samples spectrophotometer measurements of bacteria optical density was used. This method was reported by Haase *et al* as a technique for determining antibacterial properties of functionalized textiles [43]. The number of bacteria cells in inoculum was adjusted to 1.5 × 10⁸ cells ml⁻¹, measured by

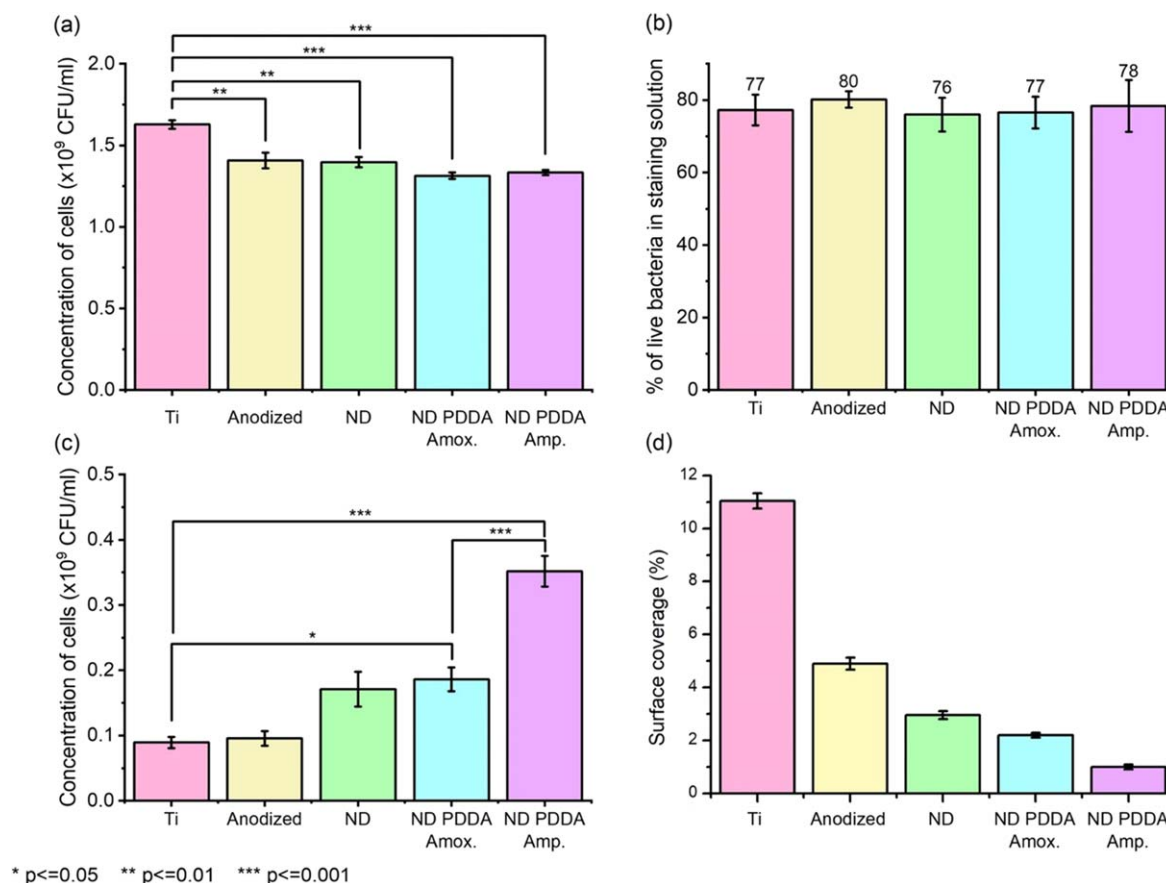


Figure 6. (a) Concentration of *E. coli* cells in the staining solutions, (b) correlated percentage of live bacteria in the staining solution after overnight staining with modified Ti, (c) concentration of *E. coli* cells in the washing solutions after rinsing, (d) surface coverage of *E. coli* after overnight incubation in bacteria solutions and flushing of the surfaces with distilled water.

absorbance at wavelength 600 nm. The bacteria solutions were placed inside the microliter plate together with Ti samples possessing various surface modifications. The number of bacteria cells within the wells after 24 h incubation, recorded from the UV-vis absorbance measurements is presented in figure 6(a). The surface of the bare and untreated Ti, had the highest number of bacteria cells $1.63 \pm 0.02 \times 10^9$ cells ml^{-1} in the well. The concentration of bacteria cells was significantly lower for the oxidized sample reaching the value $1.41 \pm 0.05 \times 10^9$ cells ml^{-1} . The formation of the oxide layer with embedded ND did not further decrease the number of bacteria cells in solution, with a value $1.4 \pm 0.05 \times 10^9$ cells ml^{-1} . Samples modified with ND conjugated with antibiotics are indicated as ND-PDDA-amoxicillin and ND-PDDA-ampicillin. They presented a significant decrease in the bacteria cell number in comparison to the bare Ti, resulting in values $1.31 \pm 0.02 \times 10^9$ cells ml^{-1} and $1.33 \pm 0.02 \times 10^9$ cells ml^{-1} respectively.

The percentage of viable bacteria in the staining solution was determined by microplate photometer after applying live/dead staining. The staining consists of two solutions SYTO[®] 9 green-fluorescent nucleic acid stain, which labels all bacteria and the red-fluorescent nucleic acid staining, which penetrates only damaged bacteria membranes [44]. All surfaces presented 77%–80% viable cells as shown in figure 6(b). No difference was observed for modified Ti

samples in comparison with unmodified. The diffusion rate of the antibiotic was too low to provide sufficient cytotoxic concentration. Due to the chemotaxis, bacteria naturally avoid contact with chemorepellents and swim towards the areas where they are not exposed to the lethal environment [45, 46]. This behavior combined with the low diffusion rate of the antibiotic from the modified surfaces explain the similar percentage of viable bacteria in the staining solutions.

In order to determine the adhesion of bacteria cells to the functionalized surfaces, the rinsing procedure was used [47]. The Ti surfaces were washed with LB medium and the absorbance of the washing solutions was measured at the wavelength of 600 nm. The results of the bacteria concentration in the washing solutions are presented in figure 6(c). The concentration of cells after rinsing of bare Ti and oxidized Ti was $0.089 \pm 0.01 \times 10^9$ cells ml^{-1} and $0.096 \pm 0.01 \times 10^9$ cells ml^{-1} respectively. The samples of ND and ND-PDDA-amoxicillin contained $0.17 \pm 0.03 \times 10^9$ cells ml^{-1} and $0.19 \pm 0.02 \times 10^9$ cells ml^{-1} respectively, showing 1.9 fold increase of bacteria concentration in the washed solution with respect to the unmodified Ti surfaces. Significant anti-adhesive properties were observed for the sample containing ND-PDDA-ampicillin. The number of washed-out cells was $0.35 \pm 0.02 \times 10^9$ cells ml^{-1} , which is 3.9 times higher than observed in the unmodified Ti surface. Bacteria attachment to the surface occurs within seconds to

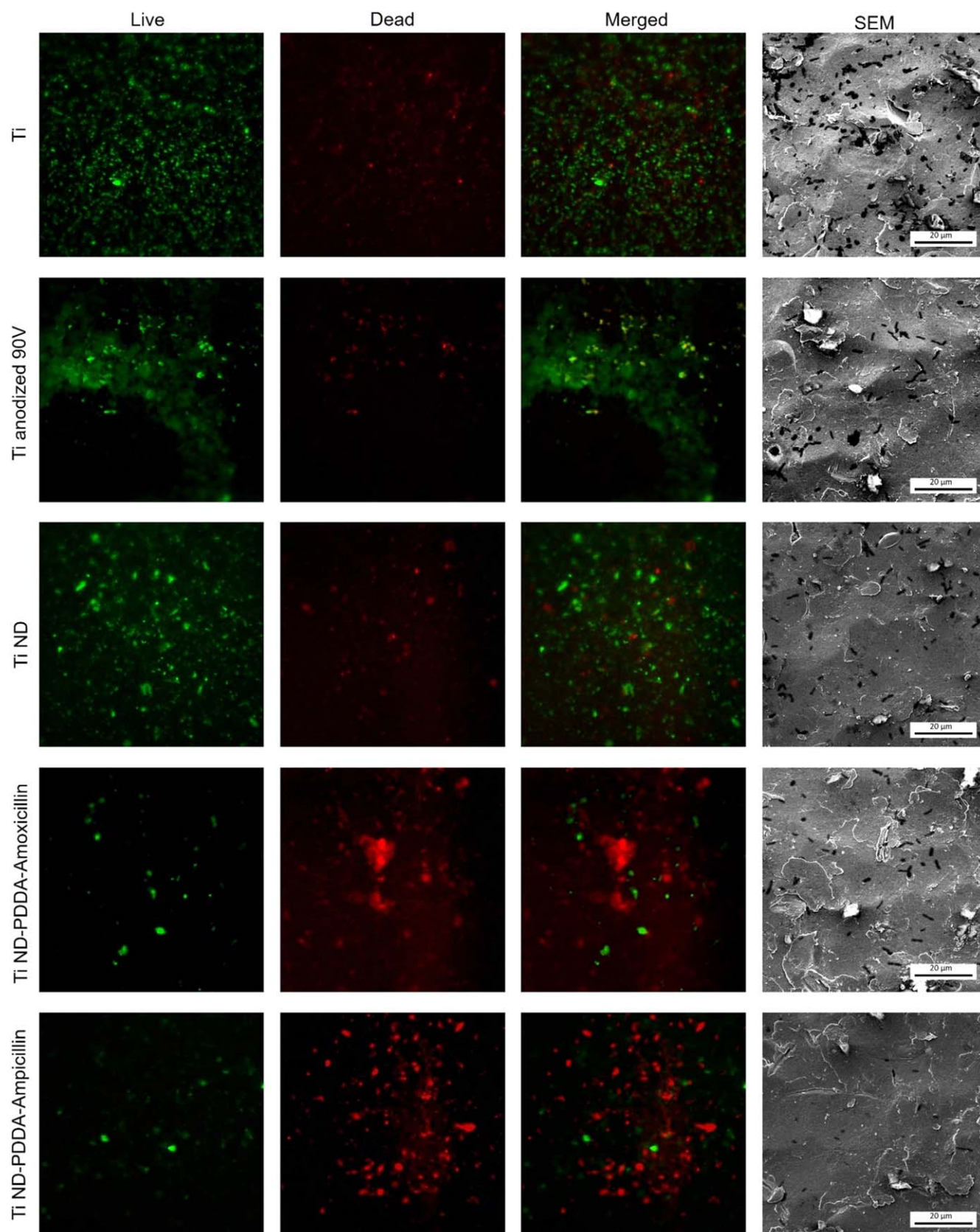


Figure 7. Assessment of antimicrobial properties of the modified surfaces. Fluorescent microscopy images of the Ti surfaces were recorded after bacteria exposure to live/dead staining. Images with green light emission indicate alive cells and with red light emission correspond to dead bacteria cells. All fluorescent microscope images were taken at 20× magnification. Correlated SEM images (right column) to assess bacteria cells coverage.

minutes after the contact with the implant surface. After a few hours bacteria start to produce extracellular polymeric substances which act as a habitat and protection from the environment and are responsible for increased bacteria survival. Detachment of bacteria during the simple washing assays from the modified surfaces indicates that after 24 h incubation, bacteria partially lost their ability to produce this protective biofilm upon the contact with the surfaces and therefore could be easily removed from the Ti samples [48].

SEM was performed to analyze the bacteria adhesion on the modified Ti surfaces. As shown in figure 6(d), bare Ti showed the highest number of attached bacteria, which covered 10.70% of the analyzed surface. *E. coli* was spread all over the surface, forming dense colonies. The surface of the oxidized Ti sample was covered by 4.97% of bacteria cells. The incorporation of ND within the oxide layer showed a reduction of bacteria coverage to 2.79%. Oxidized samples with ND conjugated with Amoxicillin had 2.26% of the sample occupied by bacteria. The lowest surface coverage and highest antimicrobial properties were obtained for ND conjugated with ampicillin, where 0.90% of the surface was covered by bacteria cells. The outcome of SEM imaging was consistent with absorbance measurements obtained from UV-vis spectroscopy, where easy detachment of the bacteria from the surface was observed for samples modified with ND-PDDA-amoxicillin and ND-PDDA-ampicillin. Decreased number of bacteria cells present on the modified surfaces combined with the high number of cells in flushed solution, indicate anti-adhesive properties of the functionalized Ti surfaces. The SEM images used for determination of surface coverage are presented in figure 7, where *E. coli* cells are represented by black hemispherical rods around 2.5 μm in length and 1 μm in width, which is consistent with the dimensions reported in the literature [49].

The live/dead staining was performed to quantify the amount of viable bacteria attached to the Ti surfaces obtained with different functionalization techniques. Upon the staining viable bacteria emit green fluorescence and dead bacteria can be distinguished by red fluorescence emission. The recorded images for green, red and merged emission are presented in figure 7. The highest number of bacteria cells on the surface was observed for the untreated and oxidized Ti. Moreover, the number of live bacteria cells in these samples was much higher than for the modified surfaces. The number of dead cells was negligible, and there was no antimicrobial effect observed.

Although the Ti sample with surface modified with ND presented a slightly increased number of dead cells, there was still a predominant amount of viable bacteria. The surface functionalization with ND conjugated with antibiotics (ND-PDDA-amoxicillin and ND-PDDA-ampicillin) showed a decreased number of live cells and a significant increase in the number of dead bacteria. The application of ND conjugated with PDDA-amoxicillin and PDDA-ampicillin resulted in a minimal number of living bacteria and a predominant number of dead cells on the Ti surface.

Bacteria clumping was observed on the surfaces of both Ti samples treated with ND conjugated to antibiotics. Bacteria clumping is a phenomenon when bacteria start to form

agglomerates to decrease the surface area that is exposed to the harmful environment [50]. Furthermore, the direct interaction of bacteria within the formed bacteria clusters, promotes the horizontal gene transfer where the acquired resistance gene from one bacterium is transferred to another via hair-like appendages called pili [51].

The diffusivity of either tested antibiotics was not sufficient to cause bacterial lethality in solution. However, the direct contact of the bacteria with the modified surfaces caused disruption of the cell walls, and bacterial death, supported by using live/dead assay. Hence, the potential application of ND modified surfaces can decrease the risk of bacterial infection at the implant-bone interface since the interface of the bone and the implant surface is the most susceptible place for the infection to occur [52, 53].

4. Conclusions





ND showed a great potential as nanocarriers of amoxicillin and ampicillin enabling the immobilization of these antibiotics within the Ti oxide layer for sustainable antimicrobial surfaces. The successful loading of amoxicillin and ampicillin onto ND surface was based on the electrostatic interactions and assessed using UV-vis spectroscopy. The electrostatic bonding enabled conjugation of small molecules such as amoxicillin with ND without loss of the antibiotic activity. The efficiency of amoxicillin binding was sufficient to enable bacteria lethality upon the contact with the modified Ti surface as examined by live/dead assay. Evaluation of the antimicrobial properties by SEM showed a decrease in the bacteria adsorption to the modified surfaces. The presented results describe a promising and controllable method for drug loading onto the Ti implant surface by using ND. The proposed Ti surface modification with ND-PDDA-amoxicillin and ND-PDDA-ampicillin shows high antimicrobial properties and could significantly decrease the need for oral antibiotic prophylaxis during the hard tissue implant surgeries.

Acknowledgments

We gratefully acknowledge the support through the International Excellence Graduate School on Emerging Materials and Processes Korea (iEGSEMP Korea) in the context of TU Dresden's Institutional Strategy (ZUK 64), funded by the Excellence Initiative of the German Federal and State Governments. The research was supported by European Social Fund (ESF) 100284305. The authors also thankfully acknowledge the laboratory facilities and support in SEM measurements provided by the Center for Regenerative Therapies Dresden. A sincere thank you to Colette Worchester for her diligent proofreading of this manuscript.

ORCID iDs

Emilia Krok  <https://orcid.org/0000-0002-4637-2729>

Sascha Balakin  <https://orcid.org/0000-0001-6169-8746>
 Jonas Jung  <https://orcid.org/0000-0002-3943-1815>
 Jörg Opitz  <https://orcid.org/0000-0003-3142-2479>
 Gianarelio Cuniberti  <https://orcid.org/0000-0002-6574-7848>

References

- [1] Zhao L, Chu P K, Zhang Y and Wu Z 2009 Antibacterial coatings on titanium implants *J. Biomed. Mater. Res. B* **91B** 470–80
- [2] Wolcott R D and Ehrlich G D 2008 Biofilms and chronic infections *JAMA-J. Am. Med. Assoc.* **299** 2682–4
- [3] El-Azizi M, Rao S, Kanchanapoom T and Khardori N 2005 *In vitro* activity of vancomycin, quinupristin/dalfopristin, and linezolid against intact and disrupted biofilms of staphylococci *Ann. Clin. Microbiol. Antimicrob.* **4**
- [4] Bratzler D W and Houck P M 2005 Antimicrobial prophylaxis for surgery: an advisory statement from the national surgical infection prevention project *Am. J. Surg.* **189** 395–404
- [5] Giannoudis P V, Parker J and Wilcox M H 2005 Methicillin-resistant *Staphylococcus aureus* in trauma and orthopaedic practice *J. Bone Joint Surg. Br.* **87-B** 755–8
- [6] Dellinger E P 2007 Prophylactic antibiotics: administration and timing before operation are more important than administration after operation *Clin. Infect. Dis.* **44** 928–30
- [7] Vaishya R, Chauhan M and Vaish A 2013 Bone cement *J. Clin. Orthop. Trauma* **4** 157–63
- [8] Yang D T, Zhang D and Arola D D 2010 Fatigue of the bone/cement interface and loosening of total joint replacements *Int. J. Fatigue* **32** 1639–49
- [9] Antoci V et al 2008 The inhibition of *Staphylococcus epidermidis* biofilm formation by vancomycin-modified titanium alloy and implications for the treatment of periprosthetic infection *Biomaterials* **29** 4684–90
- [10] Lancini G, Parenti F and Gallo G G 1995 *Antibiotics-A Multidisciplinary Approach* (Boston, MA: Springer)
- [11] Salata O V 2004 Applications of nanoparticles in biology and medicine *J. Nanobiotechnol.* **2** 1–6
- [12] Turcheniuk K and Mochalin V N 2017 Biomedical applications of nanodiamond (Review) *Nanotechnology* **28** 252001–28
- [13] Ho D, Wang C H K and Chow E K H 2015 Nanodiamonds: the intersection of nanotechnology, drug development, and personalized medicine *Sci. Adv.* **1** 1500439
- [14] Whitlow J, Pacelli S and Paul A 2017 Multifunctional nanodiamonds in regenerative medicine: recent advances and future directions *J. Control. Release* **261** 62–86
- [15] Mochalin V N, Shenderova O, Ho D and Gogotsi Y 2012 The properties and applications of nanodiamonds *Nat. Nanotechnol.* **7** 11–23
- [16] Schrand A M, Dai L, Schlager J J, Hussain S M and Osawa E 2007 Differential biocompatibility of carbon nanotubes and nanodiamonds *Diam. Relat. Mater.* **16** 2118–23
- [17] Grausova L, Bacakova L, Kromka A, Potocky S, Vanecek M, Nesladek M and Lisa V 2009 Nanodiamond as promising material for bone tissue engineering *J. Nanosci. Nanotechnol.* **9** 3524–34
- [18] Sangiao E T, Holban A M and Gestal M C 2019 Applications of nanodiamonds in the detection and therapy of infectious diseases *Materials* **12** 1639
- [19] Wehling J, Dringen R, Zare R N, Maas M and Rezwan K 2014 Bactericidal activity of partially oxidized nanodiamonds *ACS Nano* **8** 6475–83
- [20] Lee D K et al 2015 Nanodiamond-gutta percha composite biomaterials for root canal therapy *ACS Nano* **9** 11490–501
- [21] Rouhani P, Govindaraju N, Iyer J K, Kaul R, Kaul A and Singh R N 2016 Purification and functionalization of nanodiamond to serve as a platform for amoxicillin delivery *Mater. Sci. Eng. C* **63** 323–32
- [22] Balakin S, Dennison N R, Klemmed B, Spohn J, Cuniberti G, Römhildt L and Opitz J 2019 Immobilization of detonation nanodiamonds on macroscopic surfaces *Appl. Sci.* **9** 1064
- [23] Aliasghari S, Skeleton P and Thompson G E 2014 Plasma electrolytic oxidation of titanium in a phosphate/silicate electrolyte and tribological performance of the coatings *Appl. Surf. Sci.* **316** 463–76
- [24] Michael J, Beutner R, Hempel U, Scharnweber D, Worch H and Schwenzer B 2007 Surface modification of titanium-based alloys with bioactive molecules using electrochemically fixed nucleic acids *J. Biomed. Mater. Res. B* **80B** 145–55
- [25] ISO 1974 Paper—Holes for General Filing Purposes—Specifications (<https://www.iso.org/standard/5207.html>)
- [26] Schneider C A, Rasband W S and Eliceiri K W 2012 NIH Image to ImageJ: 25 years of image analysis *Nat. Methods* **9** 671–5
- [27] Krüger A, Kataoka F, Ozawa M, Fujino T, Suzuki Y, Aleksenskii A E, Vul' A Y and Osawa E 2005 Unusually tight aggregation in detonation nanodiamond: Identification and disintegration *Carbon* **43** 1722–30
- [28] Che H X, Yeap S P, Osman M S, Ahmad A L and Lim J 2014 Directed assembly of bifunctional silica-iron oxide nanocomposite with open shell structure *ACS Appl. Mater. Interfaces* **6** 16508–18
- [29] Gumustas M, Sengel-Turk C T, Gumustas A, Ozkan S A and Uslu B 2017 Effect of polymer-based nanoparticles on the assay of antimicrobial drug delivery systems *Multifunctional Systems for Combined Delivery, Biosensing and Diagnostics* (Amsterdam: Elsevier) pp 67–108
- [30] Ataklti A, Alemu K and Abebe B 2016 Study of the self-association of amoxicillin, thiamine and the hetero-association with biologically active compound chlorogenic acid *African J. Pharm. Pharmacol.* **10** 393–402
- [31] Tripathi G K, Singh S and Gupta M 2014 UV spectroscopy technique for analysis of amoxicillin trihydrate in pH stimuli sensitive formulation *Der Pharm. Sin.* **5** 29–33
- [32] Al-Uzri W A 2012 Spectrophotometric determination of amoxicillin in pharmaceutical preparations through diazotization and coupling reaction *Al-Uzri Iraqi J. Sci.* **53** 713–23
- [33] Rote A R, Kumbhoje P A and Bhambar R S 2012 UV-visible spectrophotometric simultaneous estimation of paracetamol and nabumetone by AUC method in combined tablet dosage form *Pharm. Methods* **3** 40–3
- [34] Arancibia A, Guttman J and Gonzalez C 1980 Absorption and disposition kinetics of amoxicillin in normal human subjects *Antimicrob. Agents Chemother.* **17** 199–202
- [35] Rele R V 2015 UV spectrophotometric estimation of ofloxacin by area under curve methods in bulk and pharmaceutical dosage form *Pharm. Sin.* **6** 39–43
- [36] Chuo S C, Mohd-Setapar S H, Mohamad-Aziz S N and Starov V M 2014 A new method of extraction of amoxicillin using mixed reverse micelles *Colloids Surf. A* **460** 137–44
- [37] Ali N, Teixeira J A and Addali A 2018 A review on nanofluids: fabrication, stability, and thermophysical properties *J. Nanomater.* **2018** 33
- [38] Andrews J M 2002 Determination of minimum inhibitory concentrations *J. Antimicrob. Chemother.* **48** 5–16
- [39] Palma E, Ellison L M E and G Y 2017 Calorimetric evaluation of amoxicillin stability in aqueous solutions *Mathews J. Pharm. Sci.* **2** 1–8
- [40] Peace N, Olubukola O and Moshood A 2012 Stability of reconstituted amoxicillin clavulanate potassium under simulated in-home storage conditions *J. Appl. Pharm. Sci.*

- [41] Kourmouli A, Valenti M, van Rijn E, Beaumont H J E, Kalantzi O I, Schmidt-Ott A and Biskos G 2018 Can disc diffusion susceptibility tests assess the antimicrobial activity of engineered nanoparticles? *J. Nanoparticle Res.* **20** 62
- [42] Gonçalves J P L, Shaikh A Q, Reitzig M, Kovalenko D A, Michael J, Beutner R, Cuniberti G, Scharnweber D and Opitz J 2014 Detonation nanodiamonds biofunctionalization and immobilization to titanium alloy surfaces as first steps towards medical application *Beilstein J. Org. Chem.* **10** 2765–73
- [43] Haase H, Jordan L, Keitel L, Keil C and Mahltig B 2017 Comparison of methods for determining the effectiveness of antibacterial functionalized textiles *PLoS One* **12** 16
- [44] Boulou L, Prévost M, Barbeau B, Coallier J and Desjardins R 1999 LIVE/DEAD(®) BacLight(TM): application of a new rapid staining method for direct enumeration of viable and total bacteria in drinking water *J. Microbiol. Methods* **37** 77–86
- [45] Hazelbauer G L, Falke J J and Parkinson J S 2008 Bacterial chemoreceptors: high-performance signaling in networked arrays *Trends Biochem. Sci.* **33** 9–19
- [46] Berg H C and Brown D A 1972 Chemotaxis in *Escherichia coli* analysed by three-dimensional tracking *Nature* **239** 500–4
- [47] An Y H and Friedman R J 1997 Laboratory methods for studies of bacterial adhesion *J. Microbiol. Methods* **30** 141–52
- [48] Khatoon Z, McTiernan C D, Suuronen E J, Mah T F and Alarcon E I 2018 Bacterial biofilm formation on implantable devices and approaches to its treatment and prevention *Heliyon* **4** e01067
- [49] Reshes G, Vanounou S, Fishov I and Feingold M 2008 Cell shape dynamics in *Escherichia coli* *Biophys. J.* **94** 251–64
- [50] Thornton M M, Chung-Esaki H M, Irvin C B, Bortz D M, Solomon M J and Younger J G 2012 Multicellularity and antibiotic resistance in *klebsiella pneumoniae* grown under bloodstream-mimicking fluid dynamic conditions *J. Infect. Dis.* **206** 588–95
- [51] Miller W R, Munita J M and Arias C A 2014 Mechanisms of antibiotic resistance in enterococci *Expert Rev. Anti. Infect. Ther.* **12** 1221–36
- [52] Trampuz A and Widmer A F 2006 Infections associated with orthopedic implants *Curr. Opin. Infect. Dis.* **19** 349–56
- [53] Ribeiro M, Monteiro F J and Ferraz M P 2012 Infection of orthopedic implants with emphasis on bacterial adhesion process and techniques used in studying bacterial-material interactions *Biomatter* **2** 176–94